

# ACTIVE OSMOREGULATORY ION UPTAKE ACROSS THE PLEOPODS OF THE ISOPOD *IDOTEA BALTICA* (PALLAS): ELECTROPHYSIOLOGICAL MEASUREMENTS ON ISOLATED SPLIT ENDO- AND EXOPODITES MOUNTED IN A MICRO-USSING CHAMBER

UTE POSTEL<sup>1,\*</sup>, WILHELM BECKER<sup>2</sup>, ANGELIKA BRANDT<sup>2</sup>, SUSANNE LUCK-KOPP<sup>1</sup>, SVEN RIESTENPATT<sup>1</sup>, DIRK WEIHRAUCH<sup>1</sup> AND DIETRICH SIEBERS<sup>1</sup>

<sup>1</sup>Biologische Anstalt Helgoland in der Stiftung Alfred-Wegener-Institut für Polar- und Meeresforschung, Notkestrasse 31, 22607 Hamburg, Germany and <sup>2</sup>Zoologisches Institut und Museum, Universität Hamburg, Martin-Luther-King-Platz 3, 20146 Hamburg, Germany

\*e-mail: upostel@meeresforschung.de

Accepted 26 January; published on WWW 9 March 2000

## Summary

The mechanism of active, osmoregulatory ion uptake was investigated in the pleopods of the marine isopod *Idotea baltica* (Pallas). Using isolated split half-podites of isopods acclimated to brackish water (20‰ salinity) mounted in a micro-Ussing chamber and symmetrically superfused with identical haemolymph-like salines, a mean short-circuit current  $I_{sc}$  of  $-445 \mu\text{A cm}^{-2}$  was measured in endopodites 3–5, corresponding to an inwardly directed transcellular movement of negative charge. Application of ouabain ( $5 \text{ mmol l}^{-1}$ ) to the basolateral superfusate resulted in the almost total abolition of the  $I_{sc}$  (reduced from  $-531$  to  $-47 \mu\text{A cm}^{-2}$ ), suggesting that the  $\text{Na}^+/\text{K}^+$ -ATPase is the driving force for active, electrogenic uptake of NaCl. In contrast, mean  $I_{sc}$  values close to zero were found in preparations of all exopodites and in endopodites 1 and 2. The specific activities of  $\text{Na}^+/\text{K}^+$ -ATPase corresponded with these results. Specific activities were highest in posterior endopodites 3–5 and depended on ambient salinity. In all other rami, the activities were much lower and independent of ambient salinity. Activities in posterior endopodites 3–5 were lowest in isopods acclimated to 30‰ salinity ( $2\text{--}4 \mu\text{mol P}_i \text{ mg}^{-1} \text{ protein h}^{-1}$ ), increased in individuals kept in 20‰ salinity ( $8.4 \mu\text{mol P}_i \text{ mg}^{-1} \text{ protein h}^{-1}$ ) and were

highest in isopods acclimated to 15‰ salinity ( $18.2 \mu\text{mol P}_i \text{ mg}^{-1} \text{ protein h}^{-1}$ ). When specimens were transferred from 30 to 40‰ salinity,  $\text{Na}^+/\text{K}^+$ -ATPase activity increased in the posterior endopodites. The electrophysiological and  $\text{Na}^+/\text{K}^+$ -ATPase activity measurements show that active electrogenic ion transport in this species occurs almost exclusively in posterior endopodites 3–5. The endopodite of the fifth pleopod of *I. baltica* exhibited a microscopic structure remarkably similar to that described for the lamellae of the phyllobranchiae of brachyurans. It is composed of two opposed epithelial monolayers of ionocytes, each covered by cuticle. Bundles of pillar cells are located within the ionocyte layers, which are separated by a fenestrated lamellar septum of connective tissue. The results obtained in this study indicate that endopodites 3–5 play the main role in osmoregulatory ion uptake of the isopod *I. baltica*. Moreover, the  $\text{Na}^+/\text{K}^+$ -ATPase is the only driving force behind active electrogenic ion uptake across the epithelial cells.

Key words: isopod, *Idotea baltica*, pleopod, histology, NaCl absorption,  $\text{Na}^+/\text{K}^+$ -ATPase, short-circuit current, osmoregulation.

## Introduction

Most crustaceans live in sea water. In this medium, their haemolymph is nearly iso-osmotic with respect to the environment. Thus, osmoregulation of the body fluid seems to be unnecessary. However, many species migrate to brackish or freshwater habitats. When confronted with these more dilute media, the osmotic concentration of the body fluids is hyperregulated by means of active salt uptake. For decapod crustaceans, it has been shown that this osmoregulatory ion uptake occurs predominantly in the thoracic gills (for reviews, see Mantel and Farmer, 1983; Péqueux et al., 1988; Onken et

al., 1994). In isopods, the thoracic gills are extremely reduced, and the branchial functions, including osmoregulatory active ion uptake, are located in the pleopods (Hörlyck, 1973; Bubel and Jones, 1974; Babula, 1977, 1979; Babula and Bielawski, 1981; Kümmel, 1981; Wägele, 1982). These locomotory abdominal extremities consist of thin, oval, dorsoventrally flattened leaf-like exo- and endopodites extending from the protopodite. Measurements of the activity of  $\text{Na}^+/\text{K}^+$ -ATPase, the central enzyme in active transepithelial absorption of NaCl in crustacean gills (for a review, see Towle, 1984), in the

pleopods of the euryhaline isopods *Sphaeroma serratum* (Thuet et al., 1969) and *Idotea wosnesenskii* (Holliday, 1988) indicate that active osmoregulatory ion absorption in these species is located only in the posterior endopodites. The ultrastructure of the endopodites of several osmoregulating brackish-water, freshwater and terrestrial isopods reveals characteristics typical of salt-transporting tissues, as described for the gills of other groups of crustaceans. An epithelial monolayer of ionocytes is covered by a thin cuticle. Within the cells, extensive infoldings of the apical and the interdigitating basolateral plasma membranes are closely associated with numerous elongated mitochondria (Copeland, 1968; Copeland and Fitzjarrell, 1968; Bubel and Jones, 1974; Babula, 1977, 1979; Babula and Bielawski, 1981; Kümmel, 1981; Wägele, 1982; Barra et al., 1983; Péqueux et al., 1987; Compère et al., 1989).

Two methods have been employed successfully in recent years to investigate osmoregulatory gill function in crustaceans. In decapod crustaceans, a preparation of the isolated perfused gill in combination with electrophysiological measurements of transepithelial potential difference ( $PD_{te}$ ), tracer flux studies and application of specific ion-transport inhibitors has greatly facilitated the analysis of active ion absorption across the branchial epithelium (Habas and Prosser, 1963; Croghan et al., 1965; Habas Mantel, 1967; King and Schoffeniels, 1969; Péqueux and Gilles, 1978; Siebers et al., 1985). Ten years ago, a preparation consisting of an isolated split-gill half-lamella mounted in a micro-Ussing chamber was developed (Schwarz and Graszynski, 1989) to analyze the mechanisms of active osmoregulatory ion uptake across the gills of the chinese crab *Eriocheir sinensis*. Since then, several other crab species have been investigated using this method, resulting in a more detailed knowledge of the mechanisms involved in transepithelial ion transport in these species (Schwarz, 1990; Onken and Siebers, 1992; Onken, 1996; Riestenpatt, 1995; Riestenpatt et al., 1996; Postel et al., 1998). By splitting the gill lamella, a single epithelial layer covered by an apical cuticle is obtained, allowing area-related short-circuit currents ( $I_{sc}$ ) and conductances ( $G_{te}$ ) to be measured. Moreover, advanced electrophysiological techniques such as measurements of membrane potentials using microelectrodes (Onken et al., 1991) or current fluctuation analysis (Zeiske et al., 1992) could be applied. Recently, even measurements of area-specific ion fluxes have been successfully performed in Ussing chamber experiments with crab gill epithelia (Riestenpatt, 1995; Riestenpatt et al., 1996).

Presumably because of the small dimensions of isopod pleopods and particularly the fragility of their rami, physiological experiments using perfusion techniques or split lamellae mounted in an Ussing chamber have not been attempted until now. Our interest focuses on the euryhaline valviferan isopod *Idotea baltica* (Pallas), which inhabits coastal environments with a wide range of salinities between a minimum of 3–4‰ and an upper limit of approximately 85‰ (see Sywula, 1964). In the present study, exo- and endopodites of *I. baltica* were split and mounted in a micro-

Ussing chamber, allowing electrophysiological measurements on pleopods from isopod crustaceans for the first time. Furthermore,  $Na^+/K^+$ -ATPase activity was investigated in the exo- and endopodites of isopods acclimated to different salinities. Histological investigations were included to compare the morphological organization of the podites of *I. baltica* with the structures present in the gills of crabs.

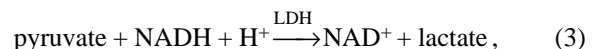
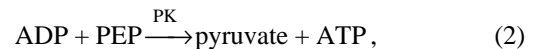
## Materials and methods

### Isopods

Isopods, *Idotea baltica* (Pallas), were caught on the rocky shore of the island of Helgoland in the North Sea. In the laboratory, they were maintained in sea water at a salinity of 30‰ and a temperature of 16 °C. Brown algae (*Ascophyllum* sp.) served as a habitat substratum and source of nutrition. Isopods were acclimated to salinities of 15, 20 and 40‰ at least 2 weeks prior to experimentation. Because of their larger body size (approximately 3 cm total length), only males were used in experiments.

### $Na^+/K^+$ -ATPase activity

The activity of the  $Na^+/K^+$ -ATPase was investigated in the endo- and exopodites of the pleopods of specimens acclimated to different salinities (15, 20, 30 and 40‰). The endo- and exopodites were of comparable size and shape, resembling an ellipse with diameters of 2 and 5 mm. The area of the podites increased from anterior to posterior, with the area of the most anterior podites being only approximately one-third of that of the most posterior podites. Because of the small size and delicate nature of the podites, their fresh masses could not be determined. Therefore, enzyme activity was normalized to the amount of protein in each individual podite. The podites were blotted of adhering water with filter paper and homogenized in a Teflon/glass Potter homogenizer (Wheaton, Millville, NJ, USA) for 1 min at 0 °C, using 200 µl of homogenizing buffer containing (in mmol l<sup>-1</sup>) 250 sucrose, 20 Tris/HCl, 20 Tris base, 2 Na<sub>2</sub>-EDTA and 0.1 % sodium deoxycholate, pH 7.6. The activity of the  $Na^+/K^+$ -ATPase was measured spectrophotometrically (Beckman, DU 65) by monitoring the absorbance at 366 nm (25 °C) in a coupled enzyme assay (Allen and Schwartz, 1969):



where ATP is adenosine triphosphate, ADP is adenosine diphosphate,  $P_i$  is inorganic phosphate, PE is phosphoenolpyruvate, NADH is reduced nicotinamide adenine dinucleotide,  $NAD^+$  is nicotinamide adenine dinucleotide, PK is pyruvate kinase and LDH is lactate dehydrogenase.

The final test volume of 1.125 ml was composed of (in mmol l<sup>-1</sup>): 100 imidazole/HCl, 150 NaCl, 100 NH<sub>4</sub>Cl, 5

MgCl<sub>2</sub>, 5 ATP, 2.5 PEP, 0.5 NADH, 20 units ml<sup>-1</sup> LDH and 5 units ml<sup>-1</sup> PK (pH 7.25). Assays were performed at 25 °C in the absence and in the presence of 5×10<sup>-3</sup> mol l<sup>-1</sup> ouabain, a specific inhibitor of the Na<sup>+</sup>/K<sup>+</sup>-ATPase that blocks its activity completely. The reduction in total ATPase activity resulting from the presence of ouabain represents Na<sup>+</sup>/K<sup>+</sup>-ATPase activity. For calculations of activity, we used the linear changes in absorbance between 5 and 15 min after starting the reaction with 0.05 ml of homogenate. The detection limit of the assays was about 0.05 μmol P<sub>i</sub> mg<sup>-1</sup> protein h<sup>-1</sup>. The method was calibrated using the commercial test for inorganic phosphate (Sigma). The protein concentrations of the homogenates were determined using a bicinchoninic acid (BCA) protein assay reagent (Pierce, Rockford, IL, USA). Homogenates were stored at -30 °C for no longer than 1 day prior to analysis of protein content.

#### *Electrophysiological measurements on podites mounted in a micro-Ussing chamber*

After the isopods had been killed by decapitation, the pleopods were excised from the abdomen under a binocular microscope (Olympus, Hamburg, Germany) and the endo- and exopodites were separated from the protopodites. For splitting, isolated podites were held in position using a pair of tweezers while a second pair of tweezers was used to draw the two facing external layers of the podites from each other. In this way, the podites were split into two half-podites, each consisting of an apical and a basolateral epithelial surface. The apical surface of one of the two half-podites is directed towards the sediment, while the apical surface of the other half-podite faces the ventral body wall of the pleon. For clarity, these epithelial layers are termed the sediment-facing and the pleon-facing half-lamella.

One half-lamella was mounted between the two half-chambers of an Ussing-type chamber modified after De Wolf and Van Driessche (1986). The half-chambers were then connected to each other using plastic screws. To minimize edge damage, silicone grease was used to seal the edges of the preparation. Using a peristaltic pump (Ismatec, Zurich, Switzerland), the chamber compartments were perfused continuously with saline (see below) at a rate of 40 ml h<sup>-1</sup>. In cases where ouabain was used, the drug was added to the basolateral saline and, in one indicated case, to the apical saline. The transepithelial potential differences ( $PD_{te}$ ) of the mounted half-podites were measured using Ag/AgCl electrodes (Mettler Toledo, Greifensee, Switzerland) connected to the chamber compartments *via* agar bridges (3% agar in 3 mmol l<sup>-1</sup> KCl). To short-circuit the  $PD_{te}$ , a second pair of electrodes serving as current electrodes connected the system to an automatic clamping device (VCC 600, Physiologic Instruments, San Diego, CA, USA) through agar bridges. The measured short-circuit current ( $I'_{sc}$ ) represents charge movement across both the salines and the preparation. To calculate the area-specific resistance ( $R'_{te}$ ) between the tips of the voltage electrodes, small induced voltage pulses (2 mV,  $\Delta PD_{te}$ ) and the resulting current deflections ( $\Delta I$ ) were used. The relatively low values of  $R_{te}$

require a correction of the  $R'_{te}$  and  $I'_{sc}$  data to obtain values for the preparation alone ( $R_{te}$ ,  $I_{sc}$ ). To determine the solution resistance ( $R_s$ ), measurements were carried out without a preparation separating the chamber compartments.

Depending on the diameter of the area between the two half-chambers used (0.7, 1.1 and 1.6 mm),  $R_s$  varied between 8.1±0.5 and 14.5±0.3 Ω cm<sup>2</sup> (means ± S.E.M.,  $N=10$ ). The corrected  $R_{te}$  was obtained by subtracting  $R_s$  from  $R'_{te}$ , while the correction of  $I'_{sc}$  followed Ohm's law. The transepithelial conductance,  $G_{te}$ , was calculated as  $G_{te}=1/R_{te}$ . In the Results section, only the corrected values are given.

#### *Histological studies*

After separation from the thorax, the pleon was immediately immersed in 6% glutaraldehyde in 0.1 mol l<sup>-1</sup> phosphate buffer, pH 7 at 4 °C. While the pleon was still immersed in this fixative, the endopodites of the fifth pleopods were excised from the protopodite and kept in the fixation solution for 24 h. Fixed endopodites were washed with phosphate buffer (0.1 mol l<sup>-1</sup>, pH 7) and then post-fixed in buffered 1% OsO<sub>4</sub> for 1 h at 4 °C. Endopodites were then washed three times for 10 min with phosphate buffer followed by dehydration in an ethanol series increasing from 35 to 100%. Samples were then treated twice for 15 min in propylene oxide before being embedded in Epon. Semi-thin (1 μm) and ultra-thin (70 nm) sections were cut with an ultramicrotome (Ultracut, Reichert-Jung, Vienna, Austria) using a glass knife and a diamond knife, respectively. For light microscopic (Olympus BH-2, Hamburg, Germany) investigation, the semi-thin sections were stained with Toluidine Blue (0.8% Toluidine Blue, 0.8% borax, 0.2% pyronin) for 1 min at 70 °C, followed by two washes with distilled water for 1 min at 70 °C. Ultra-thin sections were contrasted with uranyl acetate and lead citrate and viewed in a transmission electron microscope [EM 902, Zeiss(Leo), Oberkochen, Germany].

#### *Salines and chemicals*

To acclimate the isopods to various salinities, sea water from the North Sea was diluted with distilled water or concentrated with sea salt (Instant Ocean). The haemolymph-like saline employed in the electrophysiological measurements was composed of (in mmol l<sup>-1</sup>): 248 NaCl, 5 KCl, 5 CaCl<sub>2</sub>, 4 MgCl<sub>2</sub>, 2 NaHCO<sub>3</sub>, 5 Hepes and 2 glucose. The pH was adjusted to 7.75 with Tris before use.

#### *Statistical analyses*

All values are presented as means ± S.E.M. Differences between groups were tested using a Student's *t*-test, assuming statistical significance when  $P \leq 0.05$ .

## **Results**

#### *Na<sup>+</sup>/K<sup>+</sup>-ATPase activity*

Isopods were maintained in sea water of 30‰ salinity, and three groups were acclimated for at least 2 weeks to salinities of 15, 20 and 40‰. We did not succeed in acclimating

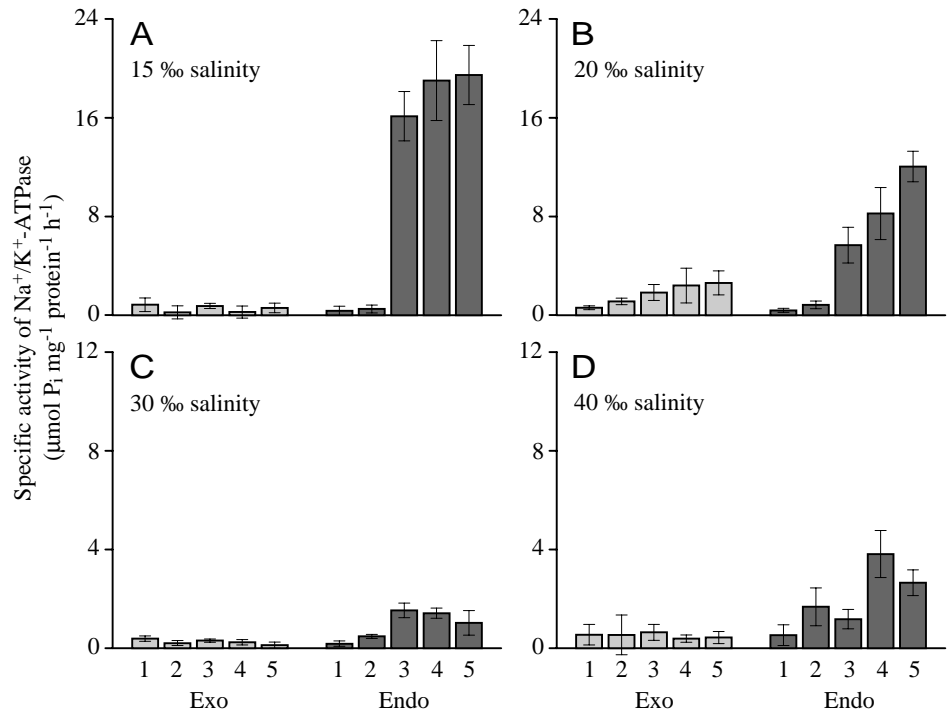


Fig. 1. Specific activity of  $\text{Na}^+/\text{K}^+$ -ATPase measured in exopodites (Exo, pale grey columns) and endopodites (Endo, dark grey columns) of the pleopods of isopods from *Idotea baltica* acclimated to various salinities. Columns represent the means  $\pm$  S.E.M.;  $N=6$  (A–C),  $N=5$  (D). Each experiment was conducted on a pooled sample of the right and left endo- or exopodites of each pair of pleopods.

specimens of *I. baltica* to salinities below 15‰. To measure  $\text{Na}^+/\text{K}^+$ -ATPase activity in the endo- and exopodites of the pleopods, the right and left endo- and exopodite, respectively, of each pair of pleopods were pooled, homogenized and analyzed for enzyme activity. In all exopodites and in the two anterior endopodites (numbers 1 and 2) of seawater-adapted (30‰ salinity) specimens,  $\text{Na}^+/\text{K}^+$ -ATPase activity was less than  $1 \mu\text{mol P}_i \text{mg}^{-1} \text{protein h}^{-1}$  (Fig. 1C). The posterior endopodites (numbers 3–5) exhibited significantly higher activities of between 2 and  $4 \mu\text{mol P}_i \text{mg}^{-1} \text{protein h}^{-1}$ . Following acclimation of isopods to brackish water of 20‰ salinity, the  $\text{Na}^+/\text{K}^+$ -ATPase activity in posterior endopodites 3–5 was greatly elevated, on average to  $8.4 \pm 1.2 \mu\text{mol P}_i \text{mg}^{-1} \text{protein h}^{-1}$  ( $N=16$ ) (Fig. 1B). Further significant increases to  $18.2 \pm 1.4 \mu\text{mol P}_i \text{mg}^{-1} \text{protein h}^{-1}$  ( $N=18$ ) were observed in posterior endopodites 3–5 of individuals acclimated to 15‰ salinity (Fig. 1A). Remarkably, an increase in the acclimation salinity to 40‰ also resulted in elevated enzyme activities in the posterior endopodites (Fig. 1D). In contrast to the high enzyme activities of posterior endopodites 3–5, which were shown to be greatly dependent on the acclimation salinity,  $\text{Na}^+/\text{K}^+$ -ATPase activities in all other podites were much lower and were independent of ambient salinity levels.

#### *Electrophysiological measurements on podites mounted in a micro-Ussing chamber*

The finding that endopodites 3–5 show enhanced  $\text{Na}^+/\text{K}^+$ -ATPase activity that is markedly dependent on ambient salinity suggests that these podites are the main sites of osmoregulatory ion absorption. To investigate further, we applied an independent methodological approach used previously by

other authors on crab gills (Schwarz and Graszynski, 1989). Isolated endo- and exopodites 1–5 were split and mounted in an Ussing-type chamber. Electrophysiological measurements were carried out while superfusing the preparation symmetrically with  $248 \text{ mmol l}^{-1}$  NaCl standard saline. To investigate the osmoregulatory abilities of the pleopods of *I. baltica*, transepithelial potential differences ( $PD_{te}$ ), short-circuit currents ( $I_{sc}$ ) and transepithelial conductances ( $G_{te}$ ) were measured in the endo- and exopodites of specimens acclimated to brackish water of 20‰ salinity. While endopodites 3–5 exhibited an inside-negative  $PD_{te}$  of  $-6.7 \pm 0.6 \text{ mV}$  ( $N=15$ ) (Fig. 2), almost no  $PD_{te}$  was generated by preparations of exopodites and endopodites 1 and 2. Among endopodites 3–5, the potential differences measured did not differ significantly. When the  $PD_{te}$  was clamped to zero, a mean  $I_{sc}$  of  $-445 \pm 34 \mu\text{A cm}^{-2}$  was observed in endopodites 3–5 ( $N=15$ ) (Fig. 2). In contrast, mean  $I_{sc}$  values close to zero were measured in all exopodites and in endopodites 1 and 2. A mean transepithelial conductance ( $G_{te}$ ) of  $84.1 \pm 4.7 \text{ mS cm}^{-2}$  was measured in the three posterior endopodites. Exopodites 2–5 and endopodites 2 showed comparable values for  $G_{te}$  ( $94.4 \pm 8.7 \text{ mS cm}^{-2}$ ,  $N=23$ ), while the first exo- and endopodites exhibited a significantly lower  $G_{te}$  of  $13.9 \pm 4.1 \text{ mS cm}^{-2}$  ( $N=8$ ). Differences in  $PD_{te}$ ,  $I_{sc}$  and  $G_{te}$  between the sediment-facing and the pleon-facing half-lamellae of endopodites 3–5 were not detectable (Fig. 3).

To determine the interrelationship between the pronounced  $\text{Na}^+/\text{K}^+$ -ATPase activities and the short-circuit currents in posterior endopodites, the effects of ouabain on  $I_{sc}$  and  $G_{te}$  of endopodites 5 of specimens acclimated to 20‰ salinity were examined. Application of ouabain ( $5 \text{ mmol l}^{-1}$ ) in the basolateral superfusate resulted in an almost total loss of  $I_{sc}$

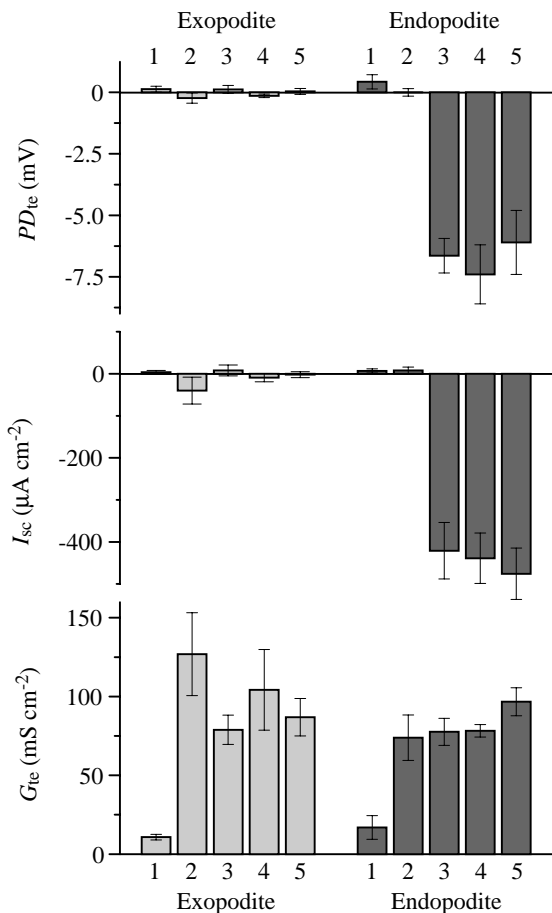


Fig. 2. Transepithelial potential differences ( $PD_{te}$ ), short-circuit currents ( $I_{sc}$ ) and transepithelial conductances ( $G_{te}$ ) measured on preparations of endo- (dark grey columns) and exopodites (pale grey columns) of pleopods mounted in an Ussing chamber. Bars represent means  $\pm$  S.E.M. from five isopods acclimated to 20‰ salinity.

from  $-531 \pm 28$  to  $-47 \pm 5 \mu A cm^{-2}$  ( $N=10$ ) (Fig. 4). Following the removal of ouabain,  $I_{sc}$  recovered to  $-226 \pm 20 \mu A cm^{-2}$ . The transepithelial conductance ( $G_{te}$ ), was only slightly sensitive to ouabain, being significantly reduced from  $85.4 \pm 3.9$  to  $75.5 \pm 2.5 mS cm^{-2}$  ( $N=10$ ) (Fig. 4). Following removal of ouabain,  $G_{te}$  did not recover but decreased further during the following 45 min to  $69.7 \pm 2.8 mS cm^{-2}$ . For a more detailed analysis of the blocking effect of ouabain, the inhibitor concentration was elevated in a stepwise fashion. In response,  $I_{sc}$  decreased in a concentration-dependent manner. Expressing the  $I_{sc}$  data as a Hanes–Woolf plot, saturation kinetics for ouabain were obtained (Fig. 5). The linear correlation ( $r=0.999$ ) of the data indicates simple Michaelis–Menten kinetics with a half-maximum inhibitor concentration  $K_{Oua}$  of  $1.3 \times 10^{-4} \pm 0.14 \times 10^{-4} mol l^{-1}$ . The maximum current decrease  $\Delta I_{max}$  is  $-545 \pm 82 \mu A cm^{-2}$ . Apical application of  $10 mmol l^{-1}$  ouabain had no effect on  $I_{sc}$  and  $G_{te}$ .

*Histological studies*

What does the procedure of splitting the podites into two

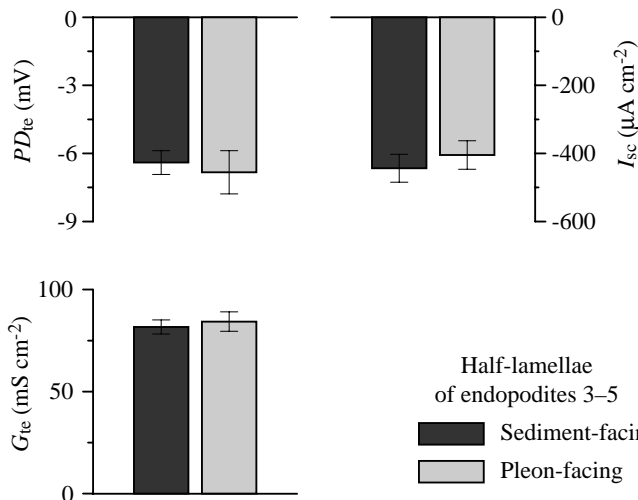


Fig. 3. Transepithelial potential differences ( $PD_{te}$ ), short-circuit currents ( $I_{sc}$ ) and transepithelial conductances ( $G_{te}$ ) measured on preparations of the sediment-facing or pleon-facing half-lamellae of posterior endopodites (3–5) mounted in an Ussing chamber. Isopods were acclimated to 20‰ salinity. Bars represent means  $\pm$  S.E.M. ( $N=15$ ).

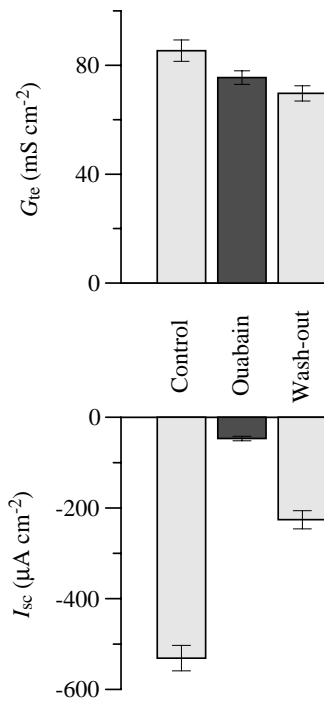
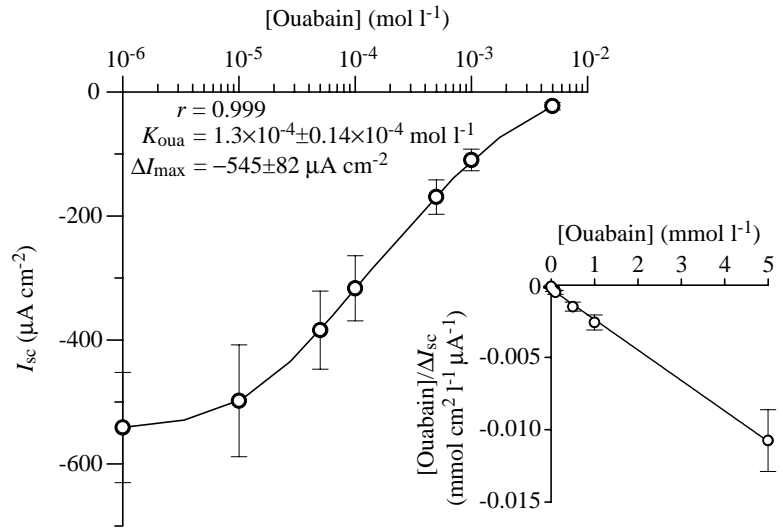


Fig. 4. Effects of basolateral ouabain ( $5 mmol l^{-1}$ ) on the short-circuit currents ( $I_{sc}$ ) and transepithelial conductances ( $G_{te}$ ) of Ussing chamber preparations of endopodite 5. Pale grey columns, controls and preparations after wash-out of ouabain; dark grey columns,  $5 mmol l^{-1}$  ouabain. Isopods were acclimated to 20‰ salinity. Bars represent means  $\pm$  S.E.M. ( $N=10$ ).

halves, to be mounted in an Ussing chamber, mean in terms of the structural organization of the gills? Histological studies were performed on pleopods using both microscopic and

Fig. 5. Dose-dependent effects of ouabain on short-circuit currents ( $I_{sc}$ ). In five experiments on different half-lamella preparations of split posterior endopodites, ouabain was added at increasing concentrations to the basolateral solution.  $I_{sc}$  (mean  $\pm$  S.E.M.) is plotted against the ouabain concentration in the basolaterally applied saline. The inset shows the same data in a Hanes–Woolf plot. The ouabain concentration is plotted against the ratio of the ouabain concentration to the respective mean ( $\pm$  S.E.M.) decrease in  $I_{sc}$  ( $[\text{ouabain}]/\Delta I_{sc}$ ). The line represents the linear regression (coefficient of correlation  $r=0.999$ ). The ouabain concentration giving a half-maximal decrease in  $I_{sc}$  ( $K_{\text{oua}}$ ) is given by the intercept of the line with the abscissa, whereas the maximum ouabain-induced decrease in current ( $\Delta I_{\text{max}}$ ) is given by the slope of the line. The mean values of  $\Delta I_{\text{max}}$  and  $K_{\text{oua}}$  were obtained from plots for the individual experiments.



ultramicroscopic techniques. To facilitate handling and to allow comparisons with electrophysiological results, the largest endopodites (number 5) were selected. As shown in Figs 6 and 7, the flattened endopodites of *I. baltica* consist of two half-lamellae of epithelial monolayers of ionocytes located opposite each other and covered by cuticle. A fenestrated lamellar septum of connective tissue was present between the sediment-facing and the pleon-facing half-lamellae. At intervals, the sediment-facing and the pleon-facing sides of the podites are connected by bundles of opposed pillar cells forming column-like structures.

The ionocytes of the epithelial layer exhibit three structurally different zones. An apical region located directly under the cuticle is characterized by numerous infoldings of the apical plasma membrane (zone 1) (Fig. 8). On the cytosolic sides of the folds, the distances between the plasma membranes often increase to form bleb-like endings which enlarge the extended subcuticular space between the folds. Numerous mitochondria are concentrated in the middle zone (zone 2) consisting of a relatively homogeneous cytoplasm without infoldings. The mitochondria are often elongated, and most of them are closely associated with the cytoplasmic endings of the apical folds. A few of them are found in close contact with basolateral invaginations. In the areas located close to the apical and basolateral cell surfaces, the folds are almost free of mitochondria. Occasional vesicle-like structures are located in the cytoplasmic region. The basolateral region (zone 3) shows many interdigitations of the plasma membranes of adjacent cells. This area is separated from the haemolymph

space by a basal lamina. The infoldings of the apical and basolateral plasma membranes are located at right angles to the side of the cell (Fig. 8). The comparatively large cells of the lamellar septum in which, in contrast to the ionocytes, the apical and the basolateral sides cannot be distinguished contain numerous glycogen granules (not illustrated). This tissue separates the extracellular space into an upper and a lower sinus containing the circulating haemolymph.

The pillar cells (Figs 6, 7, 9) traverse the whole epithelium. Their apical sides adjoin the cuticle and are structured in the same way as the ionocytes, with numerous elongated mitochondria located within the perpendicular infoldings of the strongly invaginated plasma membranes. In the region of their basal sides, the two facing groups of pillar cells penetrate the lamellar septum and contact in the middle of the connective tissue in a zone characterized by dense bundles of microtubules forming a zig-zag junctional complex.

## Discussion

### $\text{Na}^+/\text{K}^+$ -ATPase activity

The highest  $\text{Na}^+/\text{K}^+$ -ATPase specific activities detected in the posterior endopodites of isopods acclimated to 15‰ salinity were roughly  $20 \mu\text{mol P}_i \text{mg}^{-1} \text{protein h}^{-1}$ . Comparable specific activities have been found in the posterior gills of shore crabs *Carcinus maenas* acclimated to salinities of 10 and 20‰ (Siebers et al., 1982). The central role of the enzyme as the driving force in the active osmoregulatory net ion uptake of crabs has been demonstrated by tracer flux experiments



Fig. 6. Transverse semi-thin section of pleopod endopodite 5 of a specimen adapted to 30‰ salinity. The flattened endopodite consists of two epithelial monolayers (e) covered by cuticle (c). It is laterally expanded as a marginal canal (mc). A fenestrated lamellar septum (s) divides the haemolymph spaces (hs) into an upper and a lower sinus. Bundles of pillar cells (p) occur at regular intervals. Scale bar, 0.25 mm.

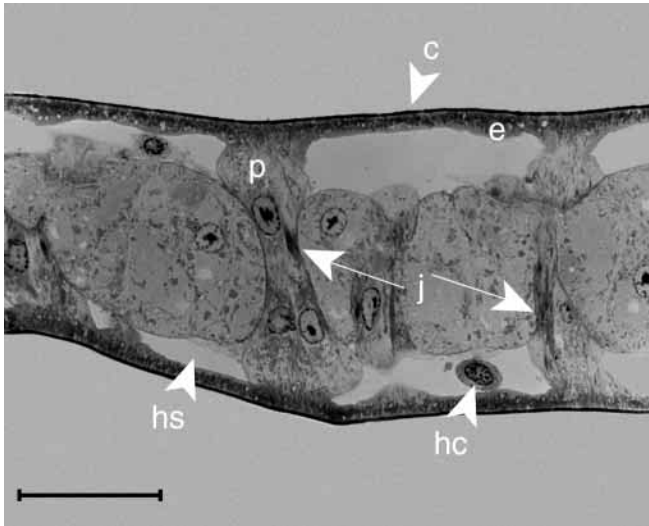


Fig. 7. Transverse semi-thin section of endopodite 5 of a specimen adapted to 30‰ salinity. The two opposite epithelial monolayers (e) of the endopodite are covered by cuticle (c). Typical cell border structures of dense bundles of microtubules (zig-zag junctions, j) are formed where two opposing pillar cells (p) meet. A laminar septum of connective tissue divides the haemolymph space (hs) into an upper and a lower sinus containing floating haemolymph cells (hc). Scale bar, 50  $\mu\text{m}$ .

(Lucu and Siebers, 1987; Riestenpatt et al., 1996). The increased activities of the  $\text{Na}^+/\text{K}^+$ -ATPase measured in the three posterior endopodites of *I. baltica* compared with activities in all the exopodites and the anterior endopodites, in combination with the large salinity-dependent alterations in activity observed only in the posterior endopodites (Fig. 1), indicate that these podites are the main sites of active osmoregulatory NaCl absorption.

This mode of distribution of  $\text{Na}^+/\text{K}^+$ -ATPase activity and its salinity-dependence has also been described in the pleopods of other isopods, e.g. *Sphaeroma serratus* (Thuet et al., 1969; Philippot et al., 1972) and *Idotea wosnesenskii* (Holliday, 1988). Our deduction of the important role of the posterior endopodites of *I. baltica* in active ion absorption corresponds with the results of silver-staining experiments performed by Hørlyck (1973), who found that, in this species, only these three podites are stained by silver and therefore considered to be permeable to chloride. As in isopods, the salinity-dependent  $\text{Na}^+/\text{K}^+$ -ATPase in various euryhaline decapods is also located in posterior branchial appendages (Mantel and Olson, 1976; Péqueux and Gilles, 1978; Spencer et al., 1979; Neufeld et al., 1980; Siebers et al., 1982).

#### *Electrophysiological measurements on podites mounted in a micro-Ussing chamber*

In the absence of any external electrophysiological driving force,  $PD_{te}$  measured in the posterior three half-endopodites superfused on both sides (symmetrically) with the same NaCl saline (Fig. 2) must be considered to be an active transport potential. The transepithelial short-circuit currents ( $I_{sc}$ )

measured under the same conditions (Fig. 2) also provides evidence for active electrogenic net ion movement (Riestenpatt et al., 1996). The polarity of the  $PD_{te}$  (inside-negative) and the negative, inwardly directed  $I_{sc}$  correspond with the findings of other authors using crab gills in Ussing chamber experiments (*Eriocheir sinensis*, Schwarz, 1990; Onken et al., 1991; Zeiske et al., 1992; Riestenpatt, 1995; *Uca tangeri*, Schwarz, 1990; *Carcinus maenas*, Onken and Siebers, 1992; Riestenpatt, 1995; Riestenpatt et al., 1996). The comparatively consistent absence of measurable  $PD_{te}$  and  $I_{sc}$  in the other podites suggests that these play little part in active osmoregulatory ion uptake. This result correlates with the distribution of  $\text{Na}^+/\text{K}^+$ -ATPase activity (Fig. 1). The dominant role of the posterior endopodites in active ion uptake is also obvious from ultrastructural investigations in the isopods *Asellus aquaticus* (Babula, 1979) and *Mesidotea entomon* (Babula and Bielawski, 1981). The strict functional differentiation within the two rami of the pleopods suggests that, besides the known morphological segmentation in arthropods, a physiological tagmatization exists in sequential organs such as pleopods. This is not immediately obvious but, as our physiological experiments suggest, is present and fully operative. The functional heterogeneity in the pleopods of isopods is remarkably similar to that described in the gills of crabs. The complete elimination of the  $I_{sc}$  in the posterior endopodites of *I. baltica* by basolateral application of ouabain (Fig. 4) corresponds with the results on posterior gills of *C. maenas* (Riestenpatt, 1995; Riestenpatt et al., 1996). In isolated posterior gills of *C. maenas*, the complete abolition of  $PD_{te}$  by ouabain coincides with the abolition of net influx of  $\text{Na}^+$  and  $\text{Cl}^-$  after treatment with this drug (Lucu and Siebers, 1987). Furthermore, the transbranchial  $I_{sc}$  measured in isolated gill half-lamellae of *C. maenas* was correlated with  $\text{Cl}^-$  influxes (Riestenpatt, 1995; Riestenpatt et al., 1996). From these and other results, it was proposed that the  $PD_{te}$  and  $I_{sc}$  measured in the gills of *C. maenas* are based on active electrogenic uptake of  $\text{Na}^+$  and  $\text{Cl}^-$  across the cells of the gill epithelium and that the underlying transport mechanism is similar to that described for the thick ascending limb of Henle's loop of the mammalian kidney. Uptake of NaCl across the apical membrane proceeds via apical  $\text{Na}^+/\text{K}^+/\text{2Cl}^-$  symport. This cotransporter is secondarily energized by the activity of the  $\text{Na}^+/\text{K}^+$ -ATPase, which generates a  $\text{Na}^+$  gradient directed into the cell. Branchial  $\text{Na}^+/\text{K}^+$ -ATPase in *C. maenas* was shown to be the only driving force energizing active, electrogenic ion uptake across this epithelium (for details, see Onken et al., 1994; Riestenpatt et al., 1996). Taken together, the pattern of  $\text{Na}^+/\text{K}^+$ -ATPase activity (Fig. 1) and the results of the Ussing chamber experiments (Figs 2, 4) suggest that the active ion uptake mechanism located in the three posterior endopodites of *I. baltica* closely resembles the coupled active electrogenic absorption of NaCl in the posterior gills of *C. maenas*.

The half-maximal inhibition of  $I_{sc}$  by basolateral ouabain ( $K_{oua}=1.3\times 10^{-4}\pm 0.14\times 10^{-4}\text{ mol l}^{-1}$ ) (Fig. 5) measured in the endopodites of *I. baltica* agrees with ouabain inhibitor

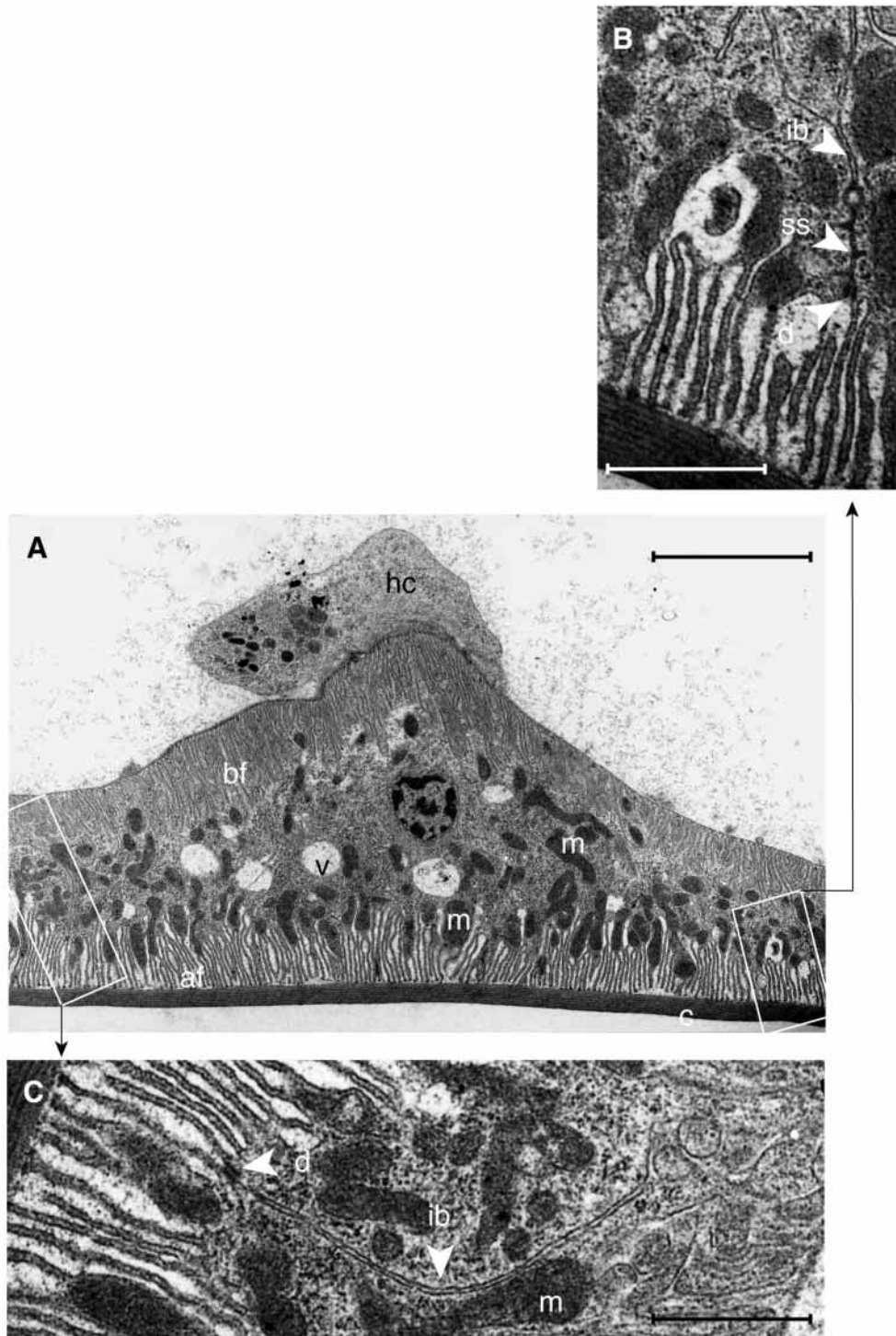


Fig. 8. (A) Transmission electron micrograph of an epithelial cell of endopodite 5 of a specimen acclimated to 20‰ salinity covered by cuticle (c) with an adjoining haemolymph cell (hc). The apical and basolateral plasma membranes form compartments of folding systems (af, apical folding system; bf, basolateral folding system) with closely related mitochondria (m). v, vesicle. Scale bar, 4  $\mu\text{m}$ . (B) Enlargement of the right-hand boxed region in A. The intercellular border (ib) shows an electron-dense sealing structure (ss) to the right of the desmosome (d). Scale bar, 1  $\mu\text{m}$ . (C) Enlargement of the left-hand boxed region in A. The intercellular border (ib) lacks septate junctions. d, desmosome; m, mitochondrion. Scale bar, 1  $\mu\text{m}$ .

constants obtained for gill tissues of other crustaceans such as *C. maenas* ( $5.6 \times 10^{-5} \text{ mol l}^{-1}$ ) (Riestenpatt et al., 1996), *E. sinensis* ( $5 \times 10^{-5}$  to  $6 \times 10^{-5} \text{ mol l}^{-1}$ ) (Schwarz and Graszynski,

1990), several species of fiddler crabs ( $7 \times 10^{-5}$  to  $8 \times 10^{-5} \text{ mol l}^{-1}$ ) (Graszynski and Bigalke, 1986), *Callinectes sapidus* ( $1.5 \times 10^{-4} \text{ mol l}^{-1}$ ) (Neufeld et al., 1980) and isopods,

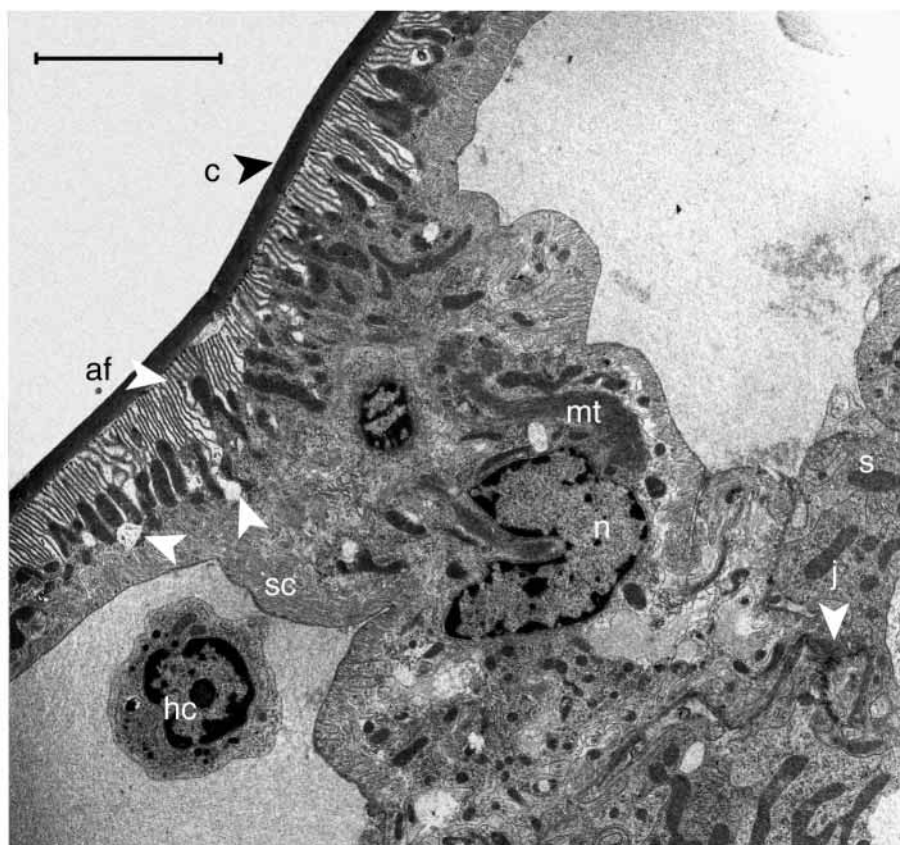


Fig. 9. Pillar cells covered by cuticle (c) are in contact with cells of the lamellar septum (s) (right side). On the left side, a haemolymph cell is visible (hc). af, apical folding system; j, zig-zag junctions; mt, bundles of microtubules; n, nucleus; sc, subcuticular space. This isopod was acclimated to 20‰ salinity. Scale bar, 5  $\mu\text{m}$ .

Table 1. Electrophysiological data on branchial epithelia of crustaceans

Species	Isolated perfused gills	Split lamellae		
	$PD_{te}$ (mV)	$PD_{te}$ (mV)	$I_{sc}$ ( $\mu\text{A cm}^{-2}$ )	$G_{te}$ ( $\text{mS cm}^{-2}$ )
<i>Idotea baltica</i>		-6.7 (1)	-445 (1)	84.1 (1)
<i>Carcinus maenas</i>	-6 to -12 (2)	-6.6 (3)	-240 (3)	40 (3)
			-375 (4)	45 (4)
<i>Eriocheir sinensis</i>	-24 (5)	Up to -40 (6)		3.2-6.8 (6)
			-64 (7)	3 (7)
			-70 (8)	3.7 (8)

Transepithelial potential differences,  $PD_{te}$  (mV), were measured in isolated perfused posterior gills of crabs.

$PD_{te}$ , short-circuit currents,  $I_{sc}$  ( $\mu\text{A cm}^{-2}$ ), and transepithelial currents  $G_{te}$  ( $\text{mS cm}^{-2}$ ), were measured in split lamellae of posterior gills of crabs and of posterior endopodites 3-5 of *I. baltica* mounted in a micro-Ussing chamber.

$PD_{te}$  and  $I_{sc}$  are given with reference to the apical side.

Crustaceans were adapted to 10‰ salinity (*C. maenas*), fresh water (*E. sinensis*) or 20‰ salinity (*I. baltica*).

Gills and half-lamellae were symmetrically exposed to haemolymph-like salines of approximately  $250 \text{ mmol l}^{-1}$  NaCl.

References are given in parentheses: 1, present study; 2, Siebers et al. (1985); 3, Onken and Siebers (1992); 4, Riestenpatt et al. (1996); 5, Péqueux and Gilles (1988); 6, Schwarz and Graszynski (1989); 7, Onken et al. (1994); 8, Riestenpatt (1995).

e.g. *S. serratum* ( $10^{-5} \text{ mol l}^{-1}$ ) (Philippot et al., 1972) and *I. wosnesenskii* ( $6.3 \times 10^{-5} \text{ mol l}^{-1}$ ) (Holliday, 1987). In general,  $\text{Na}^+/\text{K}^+$ -ATPases in crustaceans are much less ouabain-sensitive than this enzyme from mammalian tissues, which have inhibitor constants in the submicromolar range.

A comparison of electrophysiological data from the branchial epithelia of osmoregulating crustaceans (Table 1) shows that the highest transepithelial conductivity ( $G_{te}$ ) of the posterior endopodites is that of *I. baltica*. The findings indicate that the epithelium of the posterior endopodites of *I. baltica* is very leaky and allows comparatively large diffusive transepithelial losses of ions into the dilute ambient medium. These losses can only be compensated for by large ion uptake rates, as is evident from the comparatively high transepithelial short-circuit current ( $I_{sc}$ ). *I. baltica* can therefore be considered to be a comparatively moderate osmoregulator, more comparable to *C. maenas*, which cannot tolerate salinities below approximately 9‰, than to the strongly osmoregulating crab *E. sinensis* acclimated to fresh water. This deduction agrees with observations of the moderate hyperregulatory ability of *I. baltica* by Hørlyck (1973). In contrast to *I. baltica*, *E. sinensis* exhibits a much higher  $PD_{te}$  and much lower  $G_{te}$  and  $I_{sc}$  (Table 1). The ultrastructural results (see below) also demonstrate the leakiness of the epithelium of the posterior endopodites of *I. baltica* when considering the paracellular pathways in terms of intercellular junctions, which are largely lacking in septate desmosomes (Fig. 8A,B).

The results reported in this study were obtained from

specimens of *I. baltica* caught in the North Sea, which are very seldom exposed to osmotic stress. In the laboratory, these individuals could not be acclimated to salinities below 15 ‰ for periods longer than approximately 1 month. However, *I. baltica* occupies brackish-water habitats in the Baltic Sea with salinities down to 4 ‰ (Sywula, 1964). This author mentioned local populations with minimum salinity requirements of 3.06–15 ‰. Hørlyck (1973) reported difficulty in keeping specimens of this species collected in the Baltic Sea north of Helsingør in salinities below 10 ‰. A range of osmoregulatory abilities have also been reported for populations of other crustacean species, e.g. for the isopods *Gnorimosphaeroma oregonensis* (Riegel, 1959) and *Mesidotea (Saduria) entomon* (Lockwood and Croghan, 1957; Croghan and Lockwood, 1968) and for the green crab *C. maenas* (Theede, 1969). We want to emphasize that, in the present study, specimens of *I. baltica* belonging to North Sea populations were investigated because Baltic specimens, which would probably have exhibited higher levels of ion uptake, were considerably smaller, making the preparation, if feasible at all, for Ussing chamber experiments much more difficult.

#### Histological studies

The idea of splitting the rami of the pleopods of *I. baltica* and using this preparation for electrophysiological experiments in an Ussing-type chamber originated from the structural similarity between the pleopod rami of several isopod species (Babula, 1977, 1979; Babula and Bielawski, 1981; Bubel and Jones, 1974; Kümmel, 1981; Wägele, 1982) and the gill lamellae of crabs such as *C. maenas* (Goodman and Cavey, 1990) and *E. sinensis* (Barra et al., 1983), in which ion uptake has already been examined successfully using this type of experimental approach (Schwarz and Graszynski, 1989; Onken et al., 1991; Onken and Siebers, 1992; Riestenpatt, 1995; Onken, 1996; Riestenpatt et al., 1996; Postel et al., 1998). The endopodite of the fifth pleopod of *I. baltica* exhibited a microscopic structure (Fig. 8) remarkably similar to that described for the lamellae of phyllobranchiate gills of brachyurans (Drach, 1930; Copeland, 1968; Copeland and Fitzjarell, 1968; Barra et al., 1983; Cioffi, 1984; Compère et al., 1989; Goodman and Cavey, 1990; Taylor and Taylor, 1992; Lawson et al., 1994; Luquet et al., 1997).

The posterior pleopods of *I. baltica* consisted of two facing monolayers of ionocytes, each covered on the apical side by cuticle. Bundles of pillar cells located at regular intervals between the layers of ionocytes conceivably maintain the structural stability and the uniform width of the haemocoel. The ionocyte layers are separated by a fenestrated lamellar septum of connective tissue. We assume that splitting the podite resulted in the disruption of the lamellar septum and the pillar cells approximately in the area where they traverse it. According to Bubel and Jones (1974), the pleon-facing ('dorsal') side of the pleopods of the isopod *Jaera nordmanni* is folded to enclose a series of haemolymph spaces that are absent on the sediment-facing ('ventral') side. In *I. baltica*,

however, we found neither structural nor electrophysiological differences between the two epithelial sides. The absence of physiological differences (Fig. 3) between the sediment-facing and the pleon-facing half-lamellae indicates the functional homogeneity of these sides and suggests that the lamellar septum of connective tissue that remains part of the preparation during the process of splitting a podite does not contribute major polarity properties. Furthermore, we suggest that, during the preparation, the pleopod was disrupted in the region of the lamellar septum and pillar cells without major effects on the physiological functions of the epithelial monolayer. The similarity of the structural elements between crab gills and the pleopods of isopods suggests that a direct comparison of the electrophysiological data obtained from measurements on gill and pleopod half-lamellae mounted in an Ussing chamber is permissible.

This article is based on a doctoral study performed by Ute Postel at the Faculty of Biology, University of Hamburg.

#### References

- Allen, J. C. and Schwartz, A. (1969). A possible biochemical explanation for the insensitivity of the rat to cardiac glycosides. *J. Pharmac. Exp. Ther.* **168**, 42–46.
- Babula, A. (1977). Ultrastructure of gill epithelium in *Mesidotea entomon* L. (Crustacea, Isopoda). *Acta Med. Pol.* **18**, 281–282.
- Babula, A. (1979). Structure of respiratory organs of the fresh-water isopod *Asellus aquaticus* L. (Crustacea). *Bull. Soc. Amis. Sci. Lett. Poznan D Sci. Biol.* **19**, 75–82.
- Babula, A. and Bielawski, J. (1981). Ultramorphological study of gill epithelium in *Mesidotea entomon* (L.) (Isopoda, Crustacea). *Bull. Soc. Amis. Sci. Lett. Poznan D Sci. Biol.* **21**, 51–58.
- Barra, J.-A., Péqueux, A. and Humbert, W. (1983). A morphological study on gills of a crab acclimated to fresh water. *Tissue & Cell* **15**, 583–596.
- Bubel, A. and Jones, M. B. (1974). Fine structure of the gills of *Jaera nordmanni* (Rathke) (Crustacea, Isopoda). *J. Mar. Biol. Ass. UK* **54**, 737–743.
- Cioffi, M. (1984). Comparative ultrastructure of arthropod transporting epithelia. *Am. Zool.* **24**, 139–156.
- Compère, P., Wanson, S., Péqueux, A., Gilles, R. and Goffinet, G. (1989). Ultrastructural changes in the gill of the green crab *Carcinus maenas* in relation to the external salinity. *Tissue & Cell* **21**, 299–318.
- Copeland, D. E. (1968). Fine structure of salt and water uptake in the land-crab, *Gecarcinus lateralis*. *Am. Zool.* **8**, 417–432.
- Copeland, D. E. and Fitzjarrell, A. T. (1968). The salt absorbing cells in the gills of the blue crab (*Callinectes sapidus* Rathbun) with notes on modified mitochondria. *Z. Zellforsch.* **92**, 1–22.
- Croghan, P. C., Curra, R. A. and Lockwood, A. P. M. (1965). The electrical potential difference across the epithelium of isolated gills of the crayfish *Austropotamobius pallipes* (Lereboullet). *J. Exp. Biol.* **42**, 463–474.
- Croghan, P. C. and Lockwood, A. P. M. (1968). Ionic regulation of the Baltic and fresh-water races of the isopod *Mesidotea (Saduria) entomon* (L.). *J. Exp. Biol.* **48**, 141–158.
- De Wolf, I. and Van Driessche, W. (1986). Voltage-dependent  $Ba^{2+}$

- block of  $K^+$  channels in apical membrane of frog skin. *Am. J. Physiol.* **251**, C696–C706.
- Drach, P.** (1930). Étude sur système branchial des crustacés décapodes. *Arch. Anat. Microsc.* **26**, 83–133.
- Goodman, S. H. and Cavey, M. J.** (1990). Organisation of phyllobranchiate gill from the green shore crab *Carcinus maenas* (Crustacea, Decapoda). *Cell Tissue Res.* **260**, 495–505.
- Graszynski, K. and Bigalke, T.** (1986). Osmoregulation and ion transport in the extremely euryhaline fiddler crabs *Uca pugilator* and *Uca tangeri* (Ocypodidae). *Zool. Beitr. NF* **30**, 339–358.
- Habas, L. and Prosser, C. L.** (1963). The effect of acclimation to various salinities on potentials in isolated crab gills (Abstract). *Biol. Bull.* **125**, 379.
- Habas Mantel, L.** (1967). Asymmetry potentials, metabolism and sodium fluxes in gills of the blue crab, *Callinectes sapidus*. *Comp. Biochem. Physiol.* **20**, 743–753.
- Holliday, C. W.** (1988). Branchial  $Na^+/K^+$ -ATPase and osmoregulation in the isopod *Idotea wosnesenskii*. *J. Exp. Biol.* **136**, 259–272.
- Hørlyck, V.** (1973). The osmoregulatory ability in the three species of genus *Idotea* (Isopoda, Crustacea). *Ophelia* **12**, 129–140.
- King, E. N. and Schoffeniels, E.** (1969). *In vitro* preparation of crab gill for use in ion transport studies. *Arch. Int. Physiol. Biochim.* **77**, 105–111.
- Kümmel, G.** (1981). Fine structural indications of osmoregulatory function of 'gills' in terrestrial isopods (Crustacea, Oniscoidea). *Cell Tissue Res.* **214**, 663–666.
- Lawson, S. L., Jones, M. B. and Moate, R. M.** (1994). Structural variability and distribution of cells in a posterior gill of *Carcinus maenas* (Decapoda: Brachyura). *J. Mar. Biol. Ass. UK* **74**, 771–785.
- Lockwood, A. P. M. and Croghan, P. C.** (1957). The chloride regulation of the brackish and fresh-water races of *Mesidotea entomon* (L.). *J. Exp. Biol.* **34**, 253–258.
- Lucu, C. and Siebers, D.** (1987). Linkage of  $Cl^-$  fluxes with ouabain-sensitive  $Na/K$  exchange through *Carcinus* gill epithelia. *Comp. Biochem. Physiol.* **87A**, 807–811.
- Luquet, C., Pellerano, G. and Rosa, G.** (1997). Salinity-induced changes in the fine structure of the gills of the semiterrestrial estuarine crab, *Uca uruguayensis* (Nobili, 1901) (Decapoda, Ocypodidae). *Tissue & Cell* **29**, 495–501.
- Mantel, L. H. and Farmer, L. L.** (1983). Osmotic and ionic regulation. In *The Biology of Crustacea*, vol. 5 (ed. L. H. Mantel), pp. 53–161. London, New York: Academic Press.
- Mantel, L. H. and Olson, J. R.** (1976). Studies on the  $Na^+K^+$ -activated ATPase of crab gills. *Am. Zool.* **16**, 223.
- Neufeld, G. J., Holliday, C. W. and Pritchard, J. B.** (1980). Salinity adaption of gill  $Na,K$ -ATPase in blue crab, *Callinectes sapidus*. *J. Exp. Zool.* **211**, 215–224.
- Onken, H.** (1996). Active and electrogenic absorption of  $Na^+$  and  $Cl^-$  across posterior gills of *Eriocheir sinensis*: influence of short-term osmotic variations. *J. Exp. Biol.* **199**, 901–910.
- Onken, H., Graszynski, K., Johannsen, A., Putzenlechner, M., Riestenpatt, S., Schirmer, C., Siebers, D. and Zeiske, W.** (1994). How to overcome osmotic stress? Marine crabs conquer freshwater. New insights from modern electrophysiology. *Helgoländer Meeresunters.* **49**, 715–725.
- Onken, H., Graszynski, K. and Zeiske, W.** (1991).  $Na^+$ -independent, electrogenic  $Cl^-$  uptake across the posterior gills of the Chinese crab (*Eriocheir sinensis*): Voltage clamp and microelectrode studies. *J. Comp. Physiol. B* **161**, 293–301.
- Onken, H. and Siebers, D.** (1992). Voltage-clamp measurements on single split lamellae of posterior gills of the shore crab *Carcinus maenas*. *Mar. Biol.* **114**, 385–390.
- Péqueux, A. J. R., Barra, J. A. and Gilles, R.** (1987). Sub-cuticular spaces and osmotic adaptations. In *Comparative Physiology of Environmental Adaptations*, vol. 1 (ed. R. Kirsch and B. Lalou), pp. 188–197. Eighth ESCP Conference, Strasbourg 1986. Basel: Karger.
- Péqueux, A. and Gilles, R.** (1978). Osmoregulation of the euryhaline chinese crab *Eriocheir sinensis*. Ionic transports across isolated perfused gills as related to the salinity of the environment. In *Physiology and Behaviour of Marine Organisms* (ed. D. S. McLusky and A. J. Berry), pp. 105–111. Proceedings of the Twelfth European Marine Biology Symposium, Scotland. Oxford: Pergamon Press.
- Péqueux, A. and Gilles, R.** (1988). The transepithelial potential difference of isolated perfused gills of the Chinese crab *Eriocheir sinensis* acclimated to fresh water. *Comp. Biochem. Physiol.* **89A**, 163–172.
- Péqueux, A., Gilles, R. and Marshall, W. S.** (1988).  $NaCl$  transport in gills and related structures. In *Advances in Comparative and Environmental Physiology*, vol. 1 (ed. R. Greger), pp. 2–47. Berlin, Heidelberg: Springer.
- Philippot, J., Thuet, M. and Thuet, P.** (1972). Properties of the  $(Na^+-K^+)$ -ATPase from pleopods of *Sphaeroma serratum* (Fabricius). *Comp. Biochem. Physiol.* **41B**, 231–243.
- Postel, U., Petrausch, G., Riestenpatt, S., Weihrauch, D., Malykh, J., Becker, W. and Siebers, D.** (1998). Inhibition of  $Na^+/K^+$ -ATPase and of active ion-transport functions in the gills of the shore crab *Carcinus maenas* induced by cadmium. *Mar. Biol.* **130**, 407–416.
- Riegel, J. A.** (1959). Some aspects of osmoregulation in two species of sphaeromid isopod Crustacea. *Biol. Bull.* **116**, 272–284.
- Riestenpatt, S.** (1995). *Die osmoregulatorische  $NaCl$  – Aufnahme über die Kiemen decapoder Crustaceen (Crustacea, Decapoda)*. Berlin: VWF Verlag für Wissenschaft und Forschung GmbH. 131pp.
- Riestenpatt, S., Onken, H. and Siebers, D.** (1996). Active absorption of  $Na^+$  and  $Cl^-$  across the gill epithelium of the shore crab *Carcinus maenas*: voltage-clamp and ion-flux studies. *J. Exp. Biol.* **199**, 1545–1554.
- Schwarz, H.-J.** (1990). Elektrophysiologische Untersuchungen des transepithelialen Natrium-Transportes isolierter, halbiertes Kiemenplättchen posteriorer Kiemen der Wollhandkrabbe *Eriocheir sinensis* und der Winklerkrabbe *Uca tangeri*. Dissertation, Faculty of Biology, Freie Universität Berlin, Germany. 136pp.
- Schwarz, H.-J. and Graszynski, K.** (1989). Ion transport in crab gills: A new method using isolated half platelets of *Eriocheir* gill in an Ussing-type chamber. *Comp. Biochem. Physiol.* **92A**, 601–604.
- Schwarz, H.-J. and Graszynski, K.** (1990). Characterization of  $Na^+$ -transport from posterior gills of the Chinese crab *Eriocheir sinensis* using voltage-clamp-technique. *Verh. Dt. Zool. Ges.* **83**, 555–556.
- Siebers, D., Leweck, K., Markus, H. and Winkler, A.** (1982). Sodium regulation in the shore crab *Carcinus maenas* as related to ambient salinity. *Mar. Biol.* **69**, 37–43.
- Siebers, D., Winkler, A., Lucu, C., Thedens, G. and Weichart, D.** (1985).  $Na-K$ -ATPase generates an active transport potential in the gills of the hyperregulating shore crab *Carcinus maenas*. *Mar. Biol.* **87**, 185–192.

- Spencer, A., Friedling, D. A. H. and Kamemoto, F. I.** (1979). The relationship between gill NaK-ATPase activity and osmoregulatory capacity in various crabs. *Physiol. Zool.* **52**, 1–10.
- Sywula, T.** (1964). A study on the taxonomy, ecology and the geographical distribution of species of genus *Idotea* Fabricius (Isopoda, Crustacea) in the Polish Baltic. II. Ecological and zoogeographical part. *Bull. Sci. Lett. Poznan D* **4**, 173–199.
- Taylor, H. H. and Taylor, E. W.** (1992). Gills and lungs: The exchange of gases and ions. In *Microscopic Anatomy of Invertebrates*, vol. 10, *Decapod Crustacea* (ed. F. W. Harrison and A. G. Humes), pp. 203–295. New York: Wiley-Liss.
- Theede, H.** (1969). Einige neue Aspekte bei der Osmoregulation von *Carcinus maenas*. *Mar. Biol.* **2**, 114–120.
- Thuet, M., Thuet, P. and Philippot, J.** (1969). Activité de l'ATPase ( $\text{Na}^+$ – $\text{K}^+$ ) en fonction de la morphologie et de la structure histologique des pléopodes ainsi que de la concentration du sodium de l'hémolymphe chez *Sphaeroma serratum* (Fabricius). *C.R. Acad. Sci. Paris* **269**, 233–236.
- Towle, D. W.** (1984). Membrane-bound ATPase in arthropod ion-transporting tissues. *Am. Zool.* **24**, 177–185.
- Wägele, J.-W.** (1982). Ultrastructure of pleopods of the estuarine isopod *Cyathura carinata* (Crustacea: Isopoda: Anthuridae). *Zoomorph.* **101**, 215–226.
- Zeiske, W., Onken, H., Schwarz, H.-J. and Graszynski, K.** (1992). Invertebrate epithelial  $\text{Na}^+$  channels: amiloride-induced current-noise in crab gill. *Biochim. Biophys. Acta* **1105**, 245–252.